Author: Chen, Ye; Lin, Han; Ludford-Menting, Mandy J.; Clayton, Andrew H.; Gu, Min; Russell, Sarah M.
Title: Polarization of excitation light influences molecule counting in single-molecule localization microscopy
Year: 2015
Journal: Histochemistry and Cell Biology
Volume: 143
Issue: 1
Pages: 11-19
URL: http://hdl.handle.net/1959.3/392727

Polarization of excitation light influences molecule counting in single molecule localization microscopy

Ye Chen,*† Han Lin,† Mandy J. Ludford-Menting,*‡ Andrew H. Clayton,† Min Gu, † and Sarah M. Russell*†‡¶

*Immune Signalling Laboratory, Peter MacCallum Cancer Centre, East Melbourne, Australia;

†Centre for Micro-Photonics, Faculty of Science, Engineering & Technology, Swinburne University of Technology, Hawthorn, Australia;

‡ Department of Pathology, The University of Melbourne, Australia;

¶ Sir Peter MacCallum Department of Oncology, The University of Melbourne, Australia

Abstract Single molecule localization microscopy has been widely applied to count the number of biological molecules within a certain structure. The percentage of molecules that are detected significantly affects the interpretation of data. Among many factors that affect this percentage, the polarization state of the excitation light is often neglected or at least unstated in publications. We demonstrate by simulation and experiment that the number of molecules detected can be different from -40% up to 100% when using circularly- or linearly-polarized excitation light. This is determined mainly by the number of photons emitted by single fluorescent molecule, namely the choice of fluorescence proteins, and the background noise in the system, namely the illumination scheme. This difference can be further exaggerated or mitigated by various fixation methods, magnification, and camera settings We conclude that the final choice between circularly- or linearly- polarized excitation light should be made experimentally, based on the signal to noise ratio of the system.

Keywords: single molecule localization microscopy; · dSTORM; · PALM; ·polarization

Introduction

Single molecule localization microscopy, such as photoactivated localization microscopy (PALM) (Betzig, Patterson et al. 2006), using photoactivatable and photoconvertible fluorescence proteins has transformed biological imaging (Klein, Proppert et al. 2014). In addition to providing super-resolved images, this method provides information on the localization, orientation, movement and number of fluorescent molecules (Gould, Gunewardene et al. 2008), (Nair, Hosy et al. 2013). It is particularly attractive to biologists to

be able to directly count the number of molecules within a structure by imaging (Coffman and Wu 2012), providing information about the stoichiometry of a protein complex and its oligomerization state. Even for studies that are not directly aimed at counting such numbers, to retrieve as many localizations of single molecule as possible is still highly desirable, since a high Nyquist sampling ratio in many circumstances dictates the final resolution.

There are many factors that lead to either over- or under-counting in such experiments (Deschout, Shivanandan et al. 2014). Photoswitchable fluorescence proteins attached genetically to target proteins can achieve a one-to-one labeling ratio ideally. This is to assume that there is no immature fluorescence protein, complete photoconversion efficiency (Annibale, Scarselli et al. 2012, Puchner, Walter et al. 2013, Durisic, Laparra-Cuervo et al. 2014), un-labeled endogenous proteins or proteolytic cleavage, all of which would result in underestimation of the real number. On the other hand, blinking of photoswitchable fluorescence proteins (or inorganic dyes) results in overestimation, but this is normally well-accounted for, if the appropriate 'dark-frame' is allowed in data analysis (Owen, Williamson et al. 2012).

The most commonly used labels in PALM are variants of the jellyfish green fluorescent protein (GFP). Both their emission and excitation are anisotropic (Ganguly, Clayton et al. 2011). The anisotropic emission from a dipole affects the detection efficiency and the symmetry of the point spread function (Lieb, Zavislan et al. 2004, Engelhardt, Keller et al. 2011, Lew, Backlund et al. 2013, Backlund, Lew et al. 2014, Deschout, Zanacchi et al. 2014), which compromises the localization precision. When the anisotropic emission is properly analyzed, it provides molecule orientation information both in single molecule tracking (Sosa, Asenjo et al. 2010) or PALM (Gould, Gunewardene et al. 2008, Pavani, DeLuca et al. 2009).

With regard to anisotropy in excitation, inefficient excitation caused by polarization can be another cause of miss-counting molecules. This happens when a larger angle is formed between the electric field vector of the excitation light and the dipole moment of fluorescence molecules (see simulation part). The fluorophore therefore cannot emit enough photons above background to provide good signal to noise ratio (SNR), and so is not identified by algorithms in localization microscopy. It is easy to imagine that there should be an optimum illumination mode which gives the highest localization number.

Interestingly, with a few exceptions (Egner, Geisler et al. 2007, Flors, Hotta et al. 2007, Shroff, Galbraith et al. 2007), single molecule localization publications do not detail the

polarization state of their excitation light. This might be especially important for those studies aimed at counting molecules (Lando, Endesfelder et al. 2012, Puchner, Walter et al. 2013), and lack of this information could cause unnecessary difficulties in interpreting or reproducing this research. Recently, a study in which the number of subunits within a membrane protein complex with well-characterized stoichiometry was counted by steps of photo-bleaching suggested that no difference was caused by using circularly or linearly-polarize light (Durisic, Laparra-Cuervo et al. 2014). Although the authors attributed this to their particular experimental set-up, they did not rule out that polarization may affect counting in other conditions. This prompted us to formally address this issue by another approach.

MATERIALS AND METHODS

Simulation

We simulated 8100 dyes spaced evenly on a 1000×1000 grid in a 2D plane with random orientation in the field of view of 40 μm × 40 μm. The 3D orientation of a single molecule is presented as

$$\mathrm{m} = \cos\alpha\cos\beta\mathrm{i} + \sin\alpha\cos\beta\mathrm{j} + \sin\beta\mathrm{k}$$

where i, j, k are the unit vectors along the x, y and z directions, respectively. α is the angle regarding to x-axis in the sample plane (x-y plane), and β is the out-of-plane angle regarding to z-axis. As a uniform random 3D distribution is assumed, α is within the range of 0 to 2π while β is from 0 to π/2.

1. Illumination

For the epi-fluorescent simulation, we assume the incident light is a plane wave with Gaussian intensity distribution travelling along the z-axis. A linearly polarized light along the x-direction is presented as

$$\mathrm{E_L} = \mathrm{A_{Li}i}$$

A circularly polarized incident beam can be expressed as

$$\mathrm{E_C} = \frac{\sqrt{2}}{2}\mathrm{A_{Ci}}(\mathrm{i} + \mathrm{ij})$$

where $i = \sqrt{-1}$ is the complex number. A_{Li} and A_{Ci} are the amplitude distribution of the linearly and circularly polarized beam, which are equal.

For the TIRF simulation, the light is travelling from the coverglass (n_c=1.52) to water (n_w=1.33) at the incident angle θ_1=62° parallel to y-z plane.

For linearly polarized light, φ is defined as the angle between the polarization direction and the x-axis (φ = 0 for S-polarized , φ = 90° for P-polarized).

According to boundary condition when light goes through a dielectric interface (Born and Wolf 1999), the field immediately after the interface in the second media (water) becomes

$$E_{L2} = A_{Li}(t_s \cos\varphi i - t_p \sin\varphi \cos\theta_2 j + t_p \sin\varphi \sin\theta_2 k)$$

where t_s and t_p are Fresnel coefficients and $\sin\theta_2 = n_c \sin\theta_1 / n_w$ (Born and Wolf 1999).

The electric field in media2 (water) of a circularly polarized light is

$$E_{C2} = \frac{\sqrt{2}}{2} A_{Ci}[t_s i + i t_p(\cos\theta_2 j + \sin\theta_2 k)]$$

2. Fluorescence intensity

Assuming the fluorescent rate of each molecule is η, which is Gaussian statistical distribution, the fluorescent intensity of each molecule is

$$I_f = |\eta E \cdot m|^2$$

The overall intensity of each molecule is

$$I_M = I_f + I_B$$

where IB is the intensity of the background noise. A molecule was considered as identified if the signal to noise ratio was above 5 ($I_M \geq 5I_B$).

Note here under the TIRF condition, the electric fields exponentially decay in the second media with a penetration depth less than the wavelength of the incident light in free space. Therefore, we consider the molecules in a 2D plane close to the interface and use the electric field immediately after the interface in this simulation. This consideration can be applied to the 3D situation, because for the molecules deep inside (which are still within the penetration

depth of the evanescent wave) the excitation power becomes weak, equivalent to the case of low SNR. That has also been considered in the simulation.

Cell culture, constructs and immunofluorescence

HeLa cells were cultured in DMEM (Dulbecco's Modified Eagle Medium)+HEPES+5% FCS, supplemented with 1:100 Glutamate in 10% CO2 at 37 °C. MD45 cells were cultured as in (Haynes, Smyth et al. 1999). Cells were seeded on Labtek II 8-well chambered coverglass (Thermo Fisher, Waltham, MA) pre-cleaned with 5M KOH. Transfection was by Fugene6 (Promega, Fitchburg, WI) or Lipofectamine (Thermo Fisher, Waltham, MA) according to the manufacturer's instructions. pLifeAct-mEos2 was provided by Katharina Gaus and used to generate MSCV-mEos2 by PCR. PAmOrange-C1 and PAtagRFP were from Addgene (Cambridge, MA).

Cells were either fixed with 3.7 % Paraformaldehyde for 10 min, or sequentially by 0.25% and 1% glutaraldehyde in cytoskeleton buffer as described in (Rinnerthaler, Geiger et al. 1988). For indirect immunofluorescence, MD45 cells were permeabilized with 0.5% Triton-X 100 for 5 mins and probed with rabbit anti-β-PIX (Millipore, Billerica, MA) for 45 mins at R.T. and Alexa fluor 647 Donkey anti-rabbit (Thermo Fisher, Waltham, MA) for 30 mins.

Imaging

Samples were imaged on an NSTORM microscope (NIKON, Tokyo, Japan) with a 100X oil-immersion TIRF objective of numeric aperature 1.49. Less than 4 μW of a cube 405-nm laser was used for photoconversion of mEos2 or PAtagRFP, or activation of Alexa fluor 647. Less than 50 μW of a Sapphire 458-nm laser was used for photoconversion of PAmOrange. 36 mW of a Sapphire 561-nm laser was used to image the red form of mEos2, 7 or 14mW of this laser was used to image PAtagRFP, and 8 mW of a Crystalaser 647-nm laser for PAmOrange or Alexa fluor 647. All lasers were coupled into the microscope with a multi-mode fiber. The emission of mEos2 was collected through a dichroic mirror Di02-R561 and an emission filter FF01-609/57 (Semrock, Rochester, NY), the emission of PAtagRFP was collected through a dichroic mirror Di01-R405/488/561/635 and an emission filter FF01-446/523/600/677 and the emission of Alex647 or PAmOrange was collected by a built-in NIKON NSTORM filter with a band-pass filter around 660-750nm. The z-focus was maintained by the 'Perfect focusing system' using infrared light. The intensity of polarization ratios for the 561-nm laser with or without the λ/4 plate was 1:20 or 1:100, and for the 647-nm laser was 1:40 or 1:3.

The image was collected with an EMCCD camera (Andor, Belfast, Northern Ireland) (Ixon X3 Du-897 x-5633) of 256x256 pixels of a pixel size 157nm or 105nm if an additional magnification was used. Only molecules that appeared in the center 128x128 pixel of the image were used for analysis.

Imaging with photo-switchable proteins was done in phosphate buffered saline and dSTORM imaging of Alexa fluor 647 labelled proteins was done in buffers described in (Williamson, Owen et al. 2011).

Single molecule signals were identified by the ImageJ (National Institutes of Health, MD) plugin QuickPALM (Henriques, Lelek et al. 2010), with a fixed SNR of 6. The data table was then imported into MatLab (Mathworks, Natick, MA) for further analysis. We did not correct for the lateral drift since the acquisition time was short and we were only interested in counting single molecule signals per frame, not reconstructing structure. Grouping was performed for molecules appearing in 100 nm region in sequential frames and with 800 ms of dark time. All numbers shown in graph are grouped counts and the trends were the same for data without grouping.

For averaging of total number per block, the first and last 5% of frames in each block were discarded to account for the few frames when the λ/4 plate was moving or the power of activation laser was adjusted. For line plots of the number of molecules identified per frame, the curve was smoothed with a window size of 30 for better visualization. The averaged value of the first and third block was used for calculation of changes from LP to CP, which is shown together with number of repeats and standard error of mean. For histograms of signal and noise, signal was taken as the brightest pixel within the full-width-of-half-maximum (FWHM) where a single molecule was identified, and background was calculated as the average intensity in a region between 2 to 3 FWHM from the peak. The camera calibration table was then used to convert the gray value into number of photons per pixel per frame. No camera baseline was subtracted.

Results

Simulation

We simulated dipoles with random orientation in three dimensions on a plane. The simulated dipoles were excited with either circularly- polarized (CP) or linearly- polarized (LP) excitation light in epi-fluorescence (Fig1 a and b) or total internal reflection (TIR) fluorescence mode with s-, p- or mixed polarization (Fig 1 c-h). The distribution patterns of

the number of photon emitted from single dipole are largely different in CP or LP scenarios (Fig 1 a, c, e and g). CP excitation causes a peak of photon emissions in the mid-range while LP excitation leads to photon emissions that span a wider range

When noise was introduced into the system and a cut-off SNR was chosen for any given fluorephore, an effect of CP or LP on counting emerged. At low noise, fewer molecules were detected in LP mode (Fig 1b), due to the presence of a large proportion of dim molecules. When the noise increased, there was a range where the difference between those two excitation schemes was negligible, therefore the choice of polarization modes seemed to be irrelevant. Further increase in the noise level caused a sharp decrease in the number of detected molecules by CP, since only the linearly polarized excitation light can provide good alignment to a small number of dipoles, resulting in enough photon emission to be detected above very noisy background.

This result applies to both epi- and TIR-fluorescence. But in TIR mode, the effect of polarization is more complicated due to the difference between p- or s-type polarization in terms of penetration depth and orientation in the evanescent field. As a result, there are significant differences in the cut-off point where the two illumination schemes give similar results (Fig 1 d, f, h) For example, under s-polarization, LP is better than CP over a large range of noise, while under p-polarization, CP becomes superior to LP from relatively small noise. This is because the transmitted intensity of p-polarized light is higher than s-polarized light, more molecules can be found under p-polarized illumination at the same noise level due to stronger excitation.

Experimental comparison between LP and CP

To test whether similar effects occurred in biological samples, we compared the number of molecules localized under different polarization conditions in PALM imaging of HeLa cells expressing photoconvertible fluorophores. Each experiment was divided into several cycles. Within each cycle, a cell was firstly illuminated for a fixed number of frames (‘block’) under LP, then a second block with CP, and a third block with LP. The activation laser power was kept the same within each cycle but was sometimes increased for the next cycle to compensate for photo-bleaching. We only considered the results when the numbers of molecules found were similar between the first and the third block in each cycle, to ensure there was not significant run-down within this cycle.

For mEos2 fixed with glutaraldehyde and imaged under epi-fluorescence, the number of molecules identified under CP was significantly greater (increased by 64±10%, n=4） than under LP (Fig 2a). In particular, switching from LP to CP triggered a sharp increase for the first few frames, indicating that during LP excitation a pool of red species was photo-converted but not excited efficiently due to unfavorable alignment. The number of identified molecules excited by CP then declined, but was still above that of LP.

Since the SNR is mainly determined by the average photon emission from the fluorophore, we tested another photo-switchable protein, PAmOrange, that is dimmer than mEos2 (Subach, Patterson et al. 2011). PAmOrange gave the opposite trend (reduced by 38±4%, n=4） when switching from LP to CP (Fig 2b) under TIR.

Other factors modulate the difference between LP and CP

The trends were consistent in wide-field or TIR for both fluorophores but the extent to which polarization affected the counting was different: 8±3% for mEos2 by TIR and -22±4% for PAmOrange by epi-fluorescence, as well as for PAtagRFP (Subach, Patterson et al. 2010) under TIR (10±2%, n=7) or epi-fluorescence (43±4%, n=5) illumination (Fig 3). This suggests that the nature of fluorophore is most important in choosing a polarization mode which largely determines which type of polarization should be employed, while the illumination scheme, which affects background fluorescence, further modifies the magnitude of this difference. It should be noted that the quarter wave plate we used does not result in a perfectly circularly polarized light; the difference between LP and CP might be more obvious if a plate with better matching wavelength was used.

We examined other factors that could potentially affect the SNR (Fig 3). Exposure time of an EMCCD camera should match with the photon emission rate and the on-time of the fluorophore in use. We found that varying the exposure time from 40 ms to 80 ms only had a slight impact on the difference between LP and CP for both epi-fluorescence and TIRF.

The magnification of the optic system determines the pixel size of the final image. There is a trade-off between increasing the SNR level per pixel (with larger pixel size), and getting a well-spread PSF on several pixels (with smaller pixel size) (Thompson, Larson et al. 2002). It has been shown that over a relatively large range of magnification, the localization precision remain un-changed (Ober, Ram et al. 2004). To test the effect of magnification on the counting of single molecules, we compared the difference between 100X magnification (157nm per pixel) and 150X magnification (105nm per pixel). There is a dramatic increase in

counting in both epi-fluorescence and TIRF mode by using smaller pixel size (Fig 3a). This indicates that changing the magnification of the system has a great impact on the counting of single molecules.

The freedom of a fluorophore to rotate within the integrating time of the camera causes an averaging effect of both the excitation and emission. It has been shown that fixation alters the anisotropy of YFP attached to a membrane protein in cells (Ganguly, Clayton et al. 2011). Therefore, we repeated the experiment using a milder fixation, paraformaldehyde. CP still caused an increase of 13±1% (n=6) in counting compared to LP under TIR (Fig 3a) for mEos2, similar to effects with glutaraldehyde (increased by 8±3%). This indicates that both fixation methods immobilize the fluorophore enough that there is still a difference between CP and LP excitation .

When we plotted the signal and background of all the identified molecules corresponding to the experiments above (Fig 2c for mEos2, and Fig 2d for PSmOrange), we observed an increase in both signal and background when switching from LP to CP. The increase in background fluorescence could partially come from the side-lobe of the PSF of the signal itself, and partially from the other molecules (such as NADPH) whose fluorescence is less polarization dependent. Therefore, the change of SNR is eventually determined by the relative change of signal and background intensity.

This is more evident when we analyzed all data from experiments in Fig 3a, and plotted the changes of SNR from LP to CP, against the changes in molecule counting. Higher SNR in CP versus LP positively correlates with more counting (Fig 3b). Interestingly, the fitting curve crosses the y-axis at a SNR of 0.92, instead of 1. This indicates that there are other factors, together with SNR, that affect the counting. Those could be the anisotropy in emission or the dependence of photo-conversion on the polarization (which does necessarily take the same direction as excitation). It is also worth noting that by looking at only those identified molecules, we were not talking about the whole population of all potential molecules, as in our simulation.

Polarization dependence with inorganic dyes

A related single molecule localization microscopy technique to PALM is (direct) stochastic optical reconstruction microscopy or (d)STORM, which uses small inorganic dyes linked to antibodies, normally through single covalent bond. Therefore, those dyes can rotate with a higher speed and be less restrained than fluorescent proteins. Nevertheless, their rotation in space is still subject to hindrance from neighboring molecules, in a so-call orientation cone

(Engelhardt, Keller et al. 2011). The angle of this cone determines the freedom of rotation and hence the efficiency of excitation (and detection) (Backlund, Lew et al. 2014). In fact, it was reported that around 20% of dyes conjugated to antibodies absorbed on coverglass show some degree of rotation freedom (Vaughan, Jia et al. 2012).

We compared CP and LP on an Alexa fluor 647 stained dSTORM sample, but found no obvious difference (2±1%, n=3) by CP compared to LP (Fig. 3). Interestingly, we also observed an increase in photon emission when switched from LP to CP, in a manner similar to the fluorescent proteins (data not shown). This observation suggests that there is a certain degree of rigidity of those dyes attached to antibodies, but the SNR in this experiment was not in the range where a difference between CP and LP is obvious. Inorganic dyes linked to antibodies at two sites (bifunctional dyes (Corrie, Craik et al. 1998)) should have a lower freedom, so the effect of polarization excitation might be more profound.

It is worth noting that the counting by dSTORM normally does not directly translate into the number of biological molecules in the system, especially when a standard immunofluorescence protocol is employed. This is due to the multiple valency of the primary and/or secondary antibodies, the common strategy of labeling single antibody with multiple dyes to enhance the signal and blinking from the same dye. Nevertheless, comparing the relative number of localizations under different treatments still provides a good estimation of the change in the total number of molecules, especially when the labeling ratio of dye per antibody is carefully controlled (Fricke, Malkusch et al. 2014) or other means of labeling is employed (Henriques, Griffiths et al. 2011).

Conclusions

The polarization of the excitation light dramatically affects measurements of photo-convertible fluorophores, and this should be taken into account in executing and interpreting single molecule localization experiments. In general, CP should be the default configuration except in special cases when the signal to noise ratio is low, which would justify LP. The other factors such as fixation, camera exposure time, pixel size and illumination should also be optimized or taken into account when choosing whether to use CP or LP excitation.

ACKNOWLEDGMENTS

This work was supported by project grants and a fellowship from the National Health and Medical Research Foundation of Australia to SMR, and Australian Research Council Laureate Fellowship to MG and Future Fellowship to SMR. We thank Katharina Gaus for technical assistance and the pLifeAct-mEos2 construct.

Fig 1. Simulations showing the number of single molecule signals identified is affected by the polarization state of excitation light and the signal to noise ratio. (a), distribution of average photon-emission per fluorophore from a simulated pool of randomly orientated dyes in 3D excited by either linearly (thin solid line) or circularly (thick dotted line) polarized light under epi-fluorescence (a), or total internal reflection when the electric vector is at 90 (c), 45 (e), or 0 (g) degree to the incident plane. The distribution of photon emission under LP condition has a broader range than that under CP. (b, d, f, h), number of molecules identified above a SNR of 5 for those dyes in (a, c, e and g) under different noise level.

Fig 2. Experimental results showing the effect of LP or CP on counting single molecular signals. (a), number of mEos2 molecules found per frame in a single molecule localization microscopy experiment in a glutaraldehyde fixed HeLa cell under epi-fluorescence illumination. Each block is comprised of a fixed number of frames employing either LP or CP as depicted by the bars below the histogram (represented by white and black bars respectively). Every three blocks constitutes a cycle with constant activation laser power. (b), same experiment for PAmOrange in glutaraldehyde fixed HeLa cells using a total internal reflection fluorescence microscope due to the low average photon emission. An opposite trend was observed here when switching to CP. (c) and (d), normalized histogram of signal and nearby background distribution for all the identified molecules in (a) and (b), respectively. Switching from CP to LP causes increases for both signal and background but to different extents.

Fig 3. Other experimental settings further influence the magnitude of the difference between LP and CP. (a) Average change in percentage between the CP and first block of LP, or between the second and first block of LP. mEos2 in glutaraldehyde-fixed HeLa cells imaged under epi-fluorescence with 40, 60, 80 ms of exposure time or a smaller pixel size (105 nm instead of 157 nm). The increases from LP to CP were 52±2%, 65±4%, 61±4%, and 109±8% respectively (n=6). mEos2 in glutaraldehyde-fixed HeLa cells imaged by TIRFM with 40, 60,or 80 ms of exposure time or a smaller pixel size. The increases from LP to CP were

8±3%, 5±2%, 9±1%, and 22±2% respectively (n=5 or 6). mEos2-LifeAct in paraformaldehyde fixed HeLa cells imaged under TIRFM with 40, 60,or 80 ms of exposure time. The increases from LP to CP were 13±1%, 12±1%, and 10±2% respectively (n=6). PSmOrange1 in glutaraldehyde-fixed HeLa cells imaged under epi fluorescence. The decrease from LP to CP was 22±4% (n=6). Alexa fluor 647 stained β-PIX protein in paraformaldehyde fixed MD45 cells imaged under TIR. The change from LP to CP was 2±1% (n=3). For PAtagRFP in glutaraldehyde fixed HeLa cell, the increase from LP to CP was 10±2% (n=7) for 7mW excitation and 12±5% (n=5) for 14mW excitation under TIF, and 42±4% (n=5) under epi fluorescence with 7mW excitation power.(b), Dot-plot of changes in numbers of identified single molecules from LP to CP in (a), against the corresponding changes of SNR. The data were grouped by the type of proteins used and the fitting was done for all data.

References

Annibale, P., M. Scarselli, M. Greco and A. Radenovic (2012). "Identification of the factors affecting co-localization precision for quantitative multicolor localization microscopy." Optical Nanoscopy **1**(1): 9.

Backlund, M. P., M. D. Lew, A. S. Backer, S. J. Sahl and W. E. Moerner (2014). "The role of molecular dipole orientation in single-molecule fluorescence microscopy and implications for super-resolution imaging." Chemphyschem **15**(4): 587-599.

Betzig, E., G. H. Patterson, R. Sougrat, O. W. Lindwasser, S. Olenych, J. S. Bonifacino, M. W. Davidson, J. Lippincott-Schwartz and H. F. Hess (2006). "Imaging intracellular fluorescent proteins at nanometer resolution." Science **313**(5793): 1642-1645.

Born, M. and E. Wolf (1999). Principles of optics: electromagnetic theory of propagation, interference and diffraction of light, CUP Archive.

Coffman, V. C. and J. Q. Wu (2012). "Counting protein molecules using quantitative fluorescence microscopy." Trends Biochem Sci **37**(11): 499-506.

Corrie, J. E., J. S. Craik and V. R. Munasinghe (1998). "A homobifunctional rhodamine for labeling proteins with defined orientations of a fluorophore." Bioconjug Chem **9**(2): 160-167.

Deschout, H., A. Shivanandan, P. Annibale, M. Scarselli and A. Radenovic (2014). "Progress in quantitative single-molecule localization microscopy." Histochem Cell Biol **142**(1): 5-17.

Deschout, H., F. Zanacchi, M. Mlodzianoski, A. Diaspro, J. Bewersdorf, S. Hess and K. Braeckmans (2014). "Precisely and accurately localizing single emitters in fluorescence microscopy." Nature methods **11**(3): 253-266.

Durisic, N., L. Laparra-Cuervo, A. Sandoval-Álvarez, J. Borbely and M. Lakadamyali (2014). "Single-molecule evaluation of fluorescent protein photoactivation efficiency using an in vivo nanotemplate." Nature methods.

Egner, A., C. Geisler, C. von Middendorff, H. Bock, D. Wenzel, R. Medda, M. Andresen, A. C. Stiel, S. Jakobs, C. Eggeling, A. Schonle and S. W. Hell (2007). "Fluorescence nanoscopy in whole cells by asynchronous localization of photoswitching emitters." Biophys J **93**(9): 3285-3290.

Engelhardt, J., J. Keller, P. Hoyer, M. Reuss, T. Staudt and S. W. Hell (2011). "Molecular orientation affects localization accuracy in superresolution far-field fluorescence microscopy." Nano Lett **11**(1): 209-213.

Flors, C., J. Hotta, H. Uji-i, P. Dedecker, R. Ando, H. Mizuno, A. Miyawaki and J. Hofkens (2007). "A stroboscopic approach for fast photoactivation-localization microscopy with Dronpa mutants." J Am Chem Soc **129**(45): 13970-13977.
Fricke, F., S. Malkusch, G. Wangorsch, J. Greiner, B. Kaltschmidt, C. Kaltschmidt, D. Widera, T. Dandekar and M. Heilemann (2014). "Quantitative single-molecule localization microscopy combined with rule-based modeling reveals ligand-induced TNF-R1 reorganization toward higher-order oligomers." Histochemistry and cell biology.
Ganguly, S., A. H. Clayton and A. Chattopadhyay (2011). "Fixation alters fluorescence lifetime and anisotropy of cells expressing EYFP-tagged serotonin1A receptor." Biochem Biophys Res Commun **405**(2): 234-237.
Gould, T. J., M. S. Gunewardene, M. V. Gudheti, V. V. Verkhusha, S. R. Yin, J. A. Gosse and S. T. Hess (2008). "Nanoscale imaging of molecular positions and anisotropies." Nat Methods **5**(12): 1027-1030.
Haynes, N. M., M. J. Smyth, M. H. Kershaw, J. A. Trapani and P. K. Darcy (1999). "Fas-ligand-mediated lysis of erbB-2-expressing tumour cells by redirected cytotoxic T lymphocytes." Cancer Immunol Immunother **47**(5): 278-286.
Henriques, R., C. Griffiths, E. Hesper Rego and M. M. Mhlanga (2011). "PALM and STORM: unlocking live-cell super-resolution." Biopolymers **95**(5): 322-331.
Henriques, R., M. Lelek, E. F. Fornasiero, F. Valtorta, C. Zimmer and M. M. Mhlanga (2010). "QuickPALM: 3D real-time photoactivation nanoscopy image processing in ImageJ." Nat Methods **7**(5): 339-340.
Klein, T., S. Proppert and M. Sauer (2014). "Eight years of single-molecule localization microscopy." Histochemistry and cell biology.
Lando, D., U. Endesfelder, H. Berger, L. Subramanian, P. D. Dunne, J. McColl, D. Klenerman, A. M. Carr, M. Sauer, R. C. Allshire, M. Heilemann and E. D. Laue (2012). "Quantitative single-molecule microscopy reveals that CENP-A(Cnp1) deposition occurs during G2 in fission yeast." Open Biol **2**(7): 120078.
Lew, M. D., M. P. Backlund and W. E. Moerner (2013). "Rotational Mobility of Single Molecules Affects Localization Accuracy in Super-Resolution Fluorescence Microscopy." Nano Lett **13**(9): 3967-3972.
Lieb, M. A., J. M. Zavislan and L. Novotny (2004). "Single-molecule orientations determined by direct emission pattern imaging." Journal of the Optical Society of America B **21**(6): 1210-1215.
Nair, D., E. Hosy, J. D. Petersen, A. Constals, G. Giannone, D. Choquet and J. B. Sibarita (2013). "Super-resolution imaging reveals that AMPA receptors inside synapses are dynamically organized in nanodomains regulated by PSD95." J Neurosci **33**(32): 13204-13224.
Ober, R. J., S. Ram and E. S. Ward (2004). "Localization accuracy in single-molecule microscopy." Biophys J **86**(2): 1185-1200.
Owen, D. M., D. J. Williamson, A. Magenau and K. Gaus (2012). "Sub-resolution lipid domains exist in the plasma membrane and regulate protein diffusion and distribution." Nat Commun **3**: 1256.
Pavani, S. R., J. G. DeLuca and R. Piestun (2009). "Polarization sensitive, three-dimensional, single-molecule imaging of cells with a double-helix system." Opt Express **17**(22): 19644-19655.
Puchner, E., J. Walter, R. Kasper, B. Huang and W. Lim (2013). "Counting molecules in single organelles with superresolution microscopy allows tracking of the endosome maturation trajectory." Proceedings of the National Academy of Sciences of the United States of America.
Rinnerthaler, G., B. Geiger and J. V. Small (1988). "Contact formation during fibroblast locomotion: involvement of membrane ruffles and microtubules." J Cell Biol **106**(3): 747-760.
Shroff, H., C. G. Galbraith, J. A. Galbraith, H. White, J. Gillette, S. Olenych, M. W. Davidson and E. Betzig (2007). "Dual-color superresolution imaging of genetically expressed probes within individual adhesion complexes." Proc Natl Acad Sci U S A **104**(51): 20308-20313.
Sosa, H., A. B. Asenjo and E. J. Peterman (2010). "Structure and dynamics of the kinesin-microtubule interaction revealed by fluorescence polarization microscopy." Methods Cell Biol **95**: 505-519.

Subach, F. V., G. H. Patterson, M. Renz, J. Lippincott-Schwartz and V. V. Verkhusha (2010). "Bright monomeric photoactivatable red fluorescent protein for two-color super-resolution sptPALM of live cells." J Am Chem Soc **132**(18): 6481-6491.
Subach, O. M., G. H. Patterson, L. M. Ting, Y. Wang, J. S. Condeelis and V. V. Verkhusha (2011). "A photoswitchable orange-to-far-red fluorescent protein, PSmOrange." Nat Methods **8**(9): 771-777.
Thompson, R. E., D. R. Larson and W. W. Webb (2002). "Precise nanometer localization analysis for individual fluorescent probes." Biophys J **82**(5): 2775-2783.
Vaughan, J. C., S. Jia and X. Zhuang (2012). "Ultrabright photoactivatable fluorophores created by reductive caging." Nat Methods **9**(12): 1181-1184.
Williamson, D. J., D. M. Owen, J. Rossy, A. Magenau, M. Wehrmann, J. J. Gooding and K. Gaus (2011). "Pre-existing clusters of the adaptor Lat do not participate in early T cell signaling events." Nat Immunol **12**(7): 655-662.

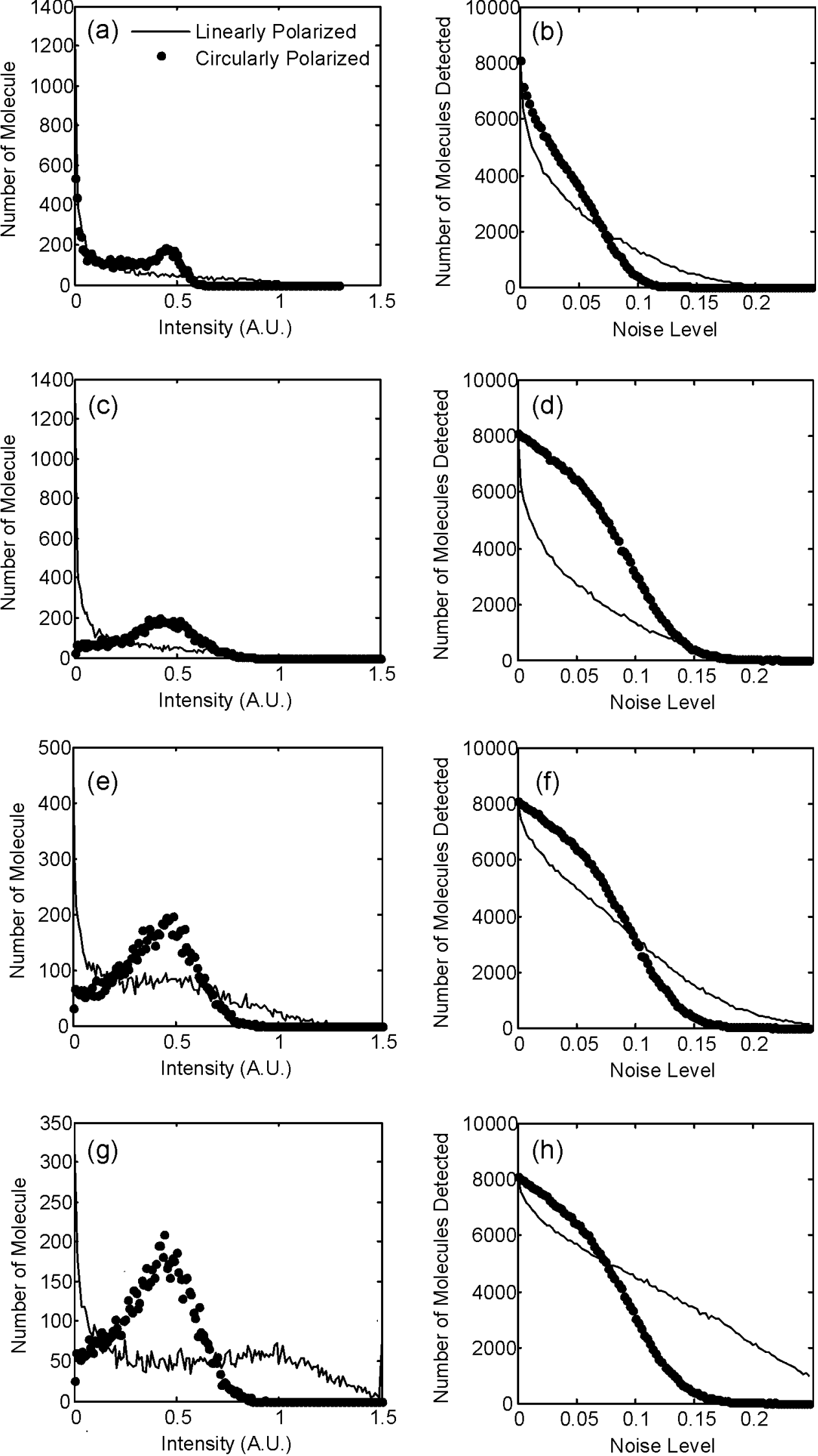
(a)
Linearly Polarized
Circularly Polarized
Number of Molecule
Intensity (A.U.)
(b)
Number of Molecules Detected
Noise Level
(c)
Number of Molecule
Intensity (A.U.)
(d)
Number of Molecules Detected
Noise Level
(e)
Number of Molecule
Intensity (A.U.)
(f)
Number of Molecules Detected
Noise Level
(g)
Number of Molecule
Intensity (A.U.)
(h)
Number of Molecules Detected
Noise Level

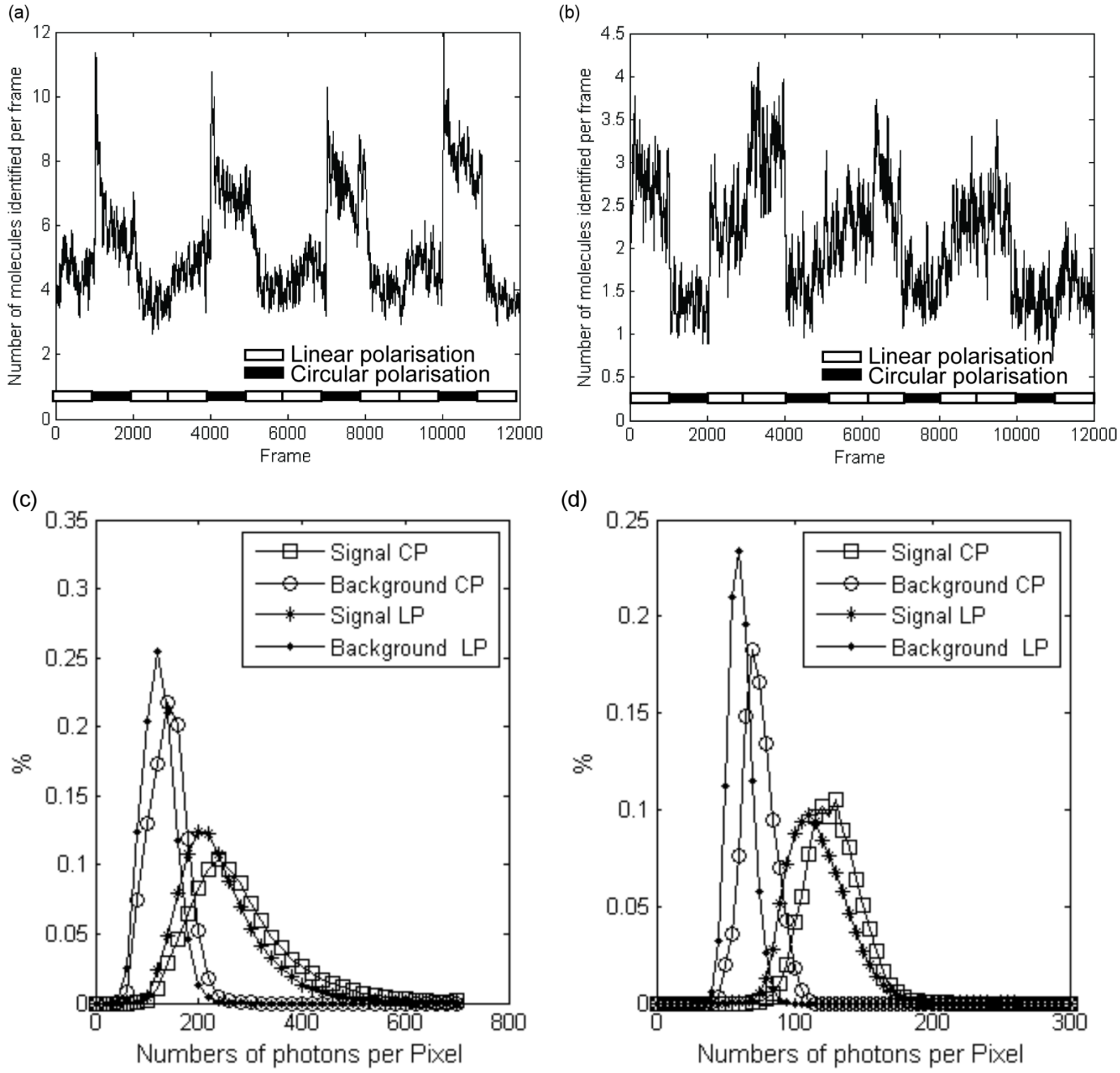
(a)
Number of molecules identified per frame
Frame
Linear polarisation
Circular polarisation
(b)
Number of molecules identified per frame
Frame
Linear polarisation
Circular polarisation

(c)
%
Numbers of photons per Pixel
Signal CP
Background CP
Signal LP
Background LP
(d)
%
Numbers of photons per Pixel
Signal CP
Background CP
Signal LP
Background LP

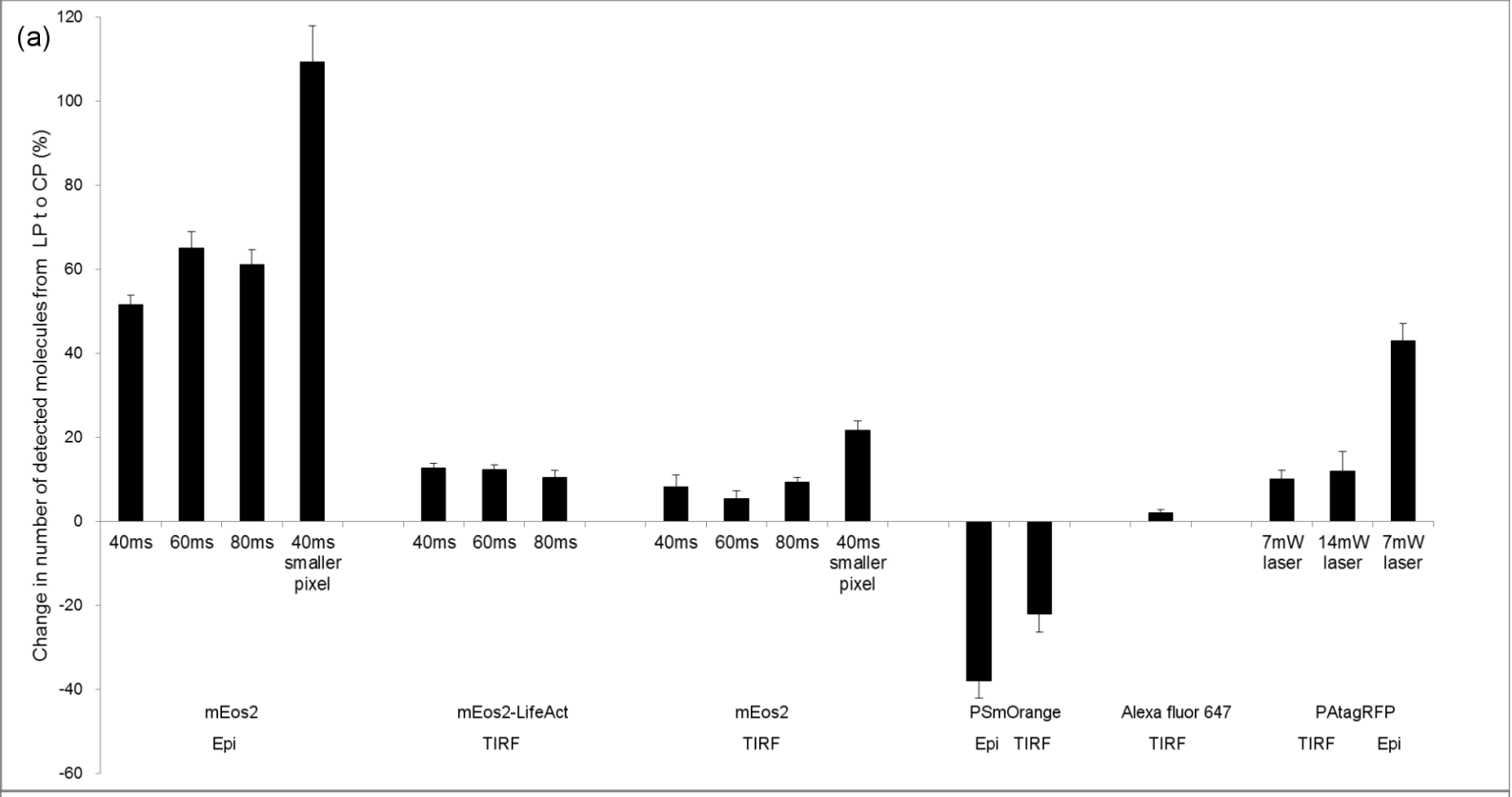
(a)
Change in number of detected molecules from LP t o CP (%)
120
100
80
60
40
20
0
-20
-40
-60
40ms
60ms
80ms
40ms smaller pixel
40ms
60ms
80ms
40ms
60ms
80ms
40ms smaller pixel
7mW laser
14mW laser
7mW laser
mEos2
Epi
mEos2-LifeAct
TIRF
mEos2
TIRF
PSmOrange
Epi
TIRF
Alexa fluor 647
TIRF
PAtagRFP
TIRF
Epi

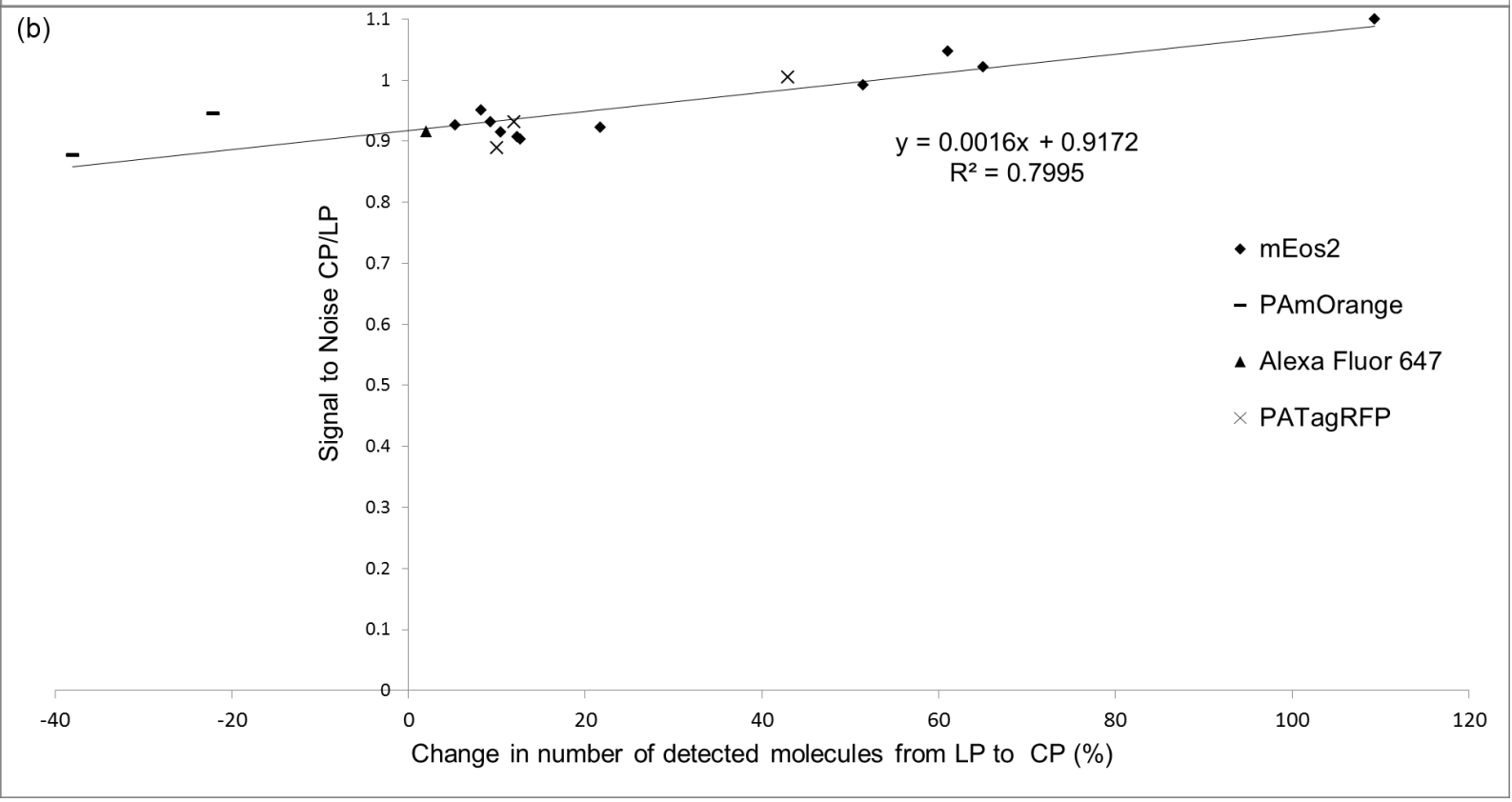
(b)
y = 0.0016x + 0.9172
R² = 0.7995
mEos2
PAmOrange
Alexa Fluor 647
PATagRFP
Signal to Noise CP/LP
1.1
1
0.9
0.8
0.7
0.6
0.5
0.4
0.3
0.2
0.1
0
-40
-20
0
20
40
60
80
100
120
Change in number of detected molecules from LP to CP (%)